Iranian Journal of Basic Medical Sciences
ijbms.mums.ac.ir

Can monomethyl fumarate and nifedipine reduce ischemia reperfusion injury in rat ovary, and what is the share of oxidative stress-sensitive transcription factors HIF-1α, NF-κB, and Nrf2?

Begum Kurt [1]*, Zeynep Deniz Sahin Inan [2], Sevgi Durna Dastan [3], Goknil Pelin Coskun [4], Ali Cetin [5]

[1] Sivas Cumhuriyet University, Faculty of Medicine, Department of Obstetrics and Gynecology, Sivas, Turkey
[2] Sivas Cumhuriyet University, Faculty of Medicine, Department of Histology & Embryology, Sivas, Turkey
[3] Sivas Cumhuriyet University, Faculty of Science, Department of Biology, Sivas, Turkey
[4] Acibadem Mehmet Ali Aydinlar University, Faculty of Pharmacy, Department of Pharmaceutical Chemistry, Istanbul, Turkey
[5] Health Sciences University, Haseki Training and Research Hospital, Department of Obstetrics and Gynecology, Istanbul, Turkey

ARTICLE INFO

Article type:
Original

Article history:
Received: Jun 30, 2025
Accepted: Dec 2, 2025

Keywords:
Experimental animal model
HIF-1α
Ischemia-reperfusion injury
NF-κB
Nrf2
Oxidative stress
Transcription factors

ABSTRACT

Objective(s): This study aimed to investigate the potential protective roles of monomethyl fumarate (MMF) and nifedipine (NF) against ovarian ischemia-reperfusion (I/R) injury in rats, with a particular focus on the contribution of oxidative stress-sensitive transcription factors HIF-1α, NF-κB, and Nrf2.

Materials and Methods: A rat model of ovarian I/R injury was established using 3-hr ischemia followed by 24-hour reperfusion. Ovarian hormone secretion capacity, oxidative stress-related biomolecular alterations, and apoptosis activation were analyzed using ELISA. Histopathological damage and apoptotic cell status were evaluated by hematoxylin-eosin (H&E) and immunohistochemical (IHC) staining. Expression levels of HIF-1α, NF-κB, Nrf2, and related downstream genes were determined using RT-qPCR.

Results: I/R significantly altered the expression of oxidative stress-associated transcription factors and their downstream targets compared with ischemia alone (P<0.05). Combined administration of MMF and NF restored serum AMH and E2 levels toward control values and reduced tissue oxidative stress markers (TOS and MDA). Gene expression of pro-apoptotic (BAX, BECLIN-1) and stress-related (HIF-1α, NF-κB, Nrf2) molecules improved under MMF and NF treatments. The combined therapy showed the most effective reduction in oxidative stress-induced molecular and histological alterations.

Conclusion: MMF and NF exerted protective effects against ovarian I/R injury by modulating oxidative stress and apoptosis. These findings suggest that the coordinated regulation of HIF-1α, NF-κB, and Nrf2 pathways may play a pivotal role in reducing reperfusion-related ovarian tissue damage.

▶ Please cite this article as:
Kurt B, Inan ZDS, Dastan SD, Coskun GP, Cetin A. Can monomethyl fumarate and nifedipine reduce ischemia reperfusion injury in rat ovary, and what is the share of oxidative stress-sensitive transcription factors HIF-1α, NF-κB, and Nrf2? Iran J Basic Med Sci 2026; 29: 446-457. doi: https://dx.doi.org/10.22038/ijbms.2026.89192.19254

Introduction

Ischaemia-Reperfusion (I/R) injury is defined as the paradoxical exacerbation of cellular dysfunction, following restoration of blood flow to previously ischaemic tissues. Reestablishment of blood flow is essential to salvage ischaemic tissues. However, reperfusion itself paradoxically causes further damage, threatening the function and viability of the organ. Reperfusion injury is a multifactorial process that results in extensive tissue destruction (1).

Ovarian torsion is a gynecological emergency that results from partial or complete rotation of the ovary around its ligamentous supports, resulting in interruption of blood flow. Prompt diagnosis and surgical treatment are essential to prevent high morbidity (2, 3). During conservative surgery, the torsioned ovary is inverted and exposed. This ensures ovarian detorsion. Subsequent I/R injury induces oxidative stress, inflammation, and apoptosis, ultimately impairing ovarian function and fertility. The reperfusion phase, rather than ischemia itself, is primarily responsible for tissue damage due to excessive production of reactive oxygen species (ROS)(4). During reperfusion, accumulated ROS interact with lipids, proteins, and nucleic acids, triggering lipid peroxidation and cellular dysfunction (5, 6). These oxidative events activate redox-sensitive transcription factors, including hypoxia-inducible factor-1 alpha (HIF-1α), nuclear factor kappa B (NF-κB), and nuclear factor erythroid 2–related factor 2 (Nrf2), which play crucial roles in regulating cellular adaptation to hypoxia, inflammation, and antioxidant defense.

HIF-1α functions as a primary hypoxia sensor, promoting cellular survival under oxygen-deprived conditions (7-9). In contrast, NF-κB is activated by oxidative stress and mediates inflammatory gene expression (10, 11). Nrf2, on the other hand, regulates the transcription of antioxidant

***Corresponding author:** Begum Kurt. Sivas Cumhuriyet University, Faculty of Medicine, Department of Obstetrics and Gynecology, Sivas, Turkey. Email: begumkurt@cumhuriyet.edu.tr

response elements and maintains redox homeostasis by modulating enzymes such as HO-1, GPx, and SOD (12, 13). Disruption of the balance between NF-κB activation and Nrf2 signaling may exacerbate oxidative injury, whereas pharmacological modulation of these pathways could confer tissue protection. Monomethyl fumarate (MMF), the active metabolite of dimethyl fumarate, is known to activate Nrf2 and suppress proinflammatory cytokines, thereby reducing oxidative stress (14, 15). Nifedipine (NF), a calcium channel blocker, has also been shown to inhibit NF-κB signaling and enhance antioxidant responses, thus providing potential synergistic protection (16, 17).

Given the shared oxidative stress–related mechanisms in reproductive ischemic injury models, combining MMF and NF may offer additive or synergistic protection by modulating HIF-1α, NF-κB, and Nrf2 pathways. However, to date, no study has comprehensively evaluated the concurrent effects of these two agents in ovarian I/R injury.

Therefore, the present study aimed to investigate the biochemical, histological, and molecular effects of MMF and NF, both alone and in combination, on ovarian I/R injury in rats, with a specific focus on oxidative stress–sensitive transcription factors HIF-1α, NF-κB, and Nrf2. The quantification of MMF and NF analysis in the ovarian tissue was also analyzed using a liquid chromatography–mass spectrometry (LC–MS) system.

Materials and Methods

Animals and experimental design

52 newly adult, unmated, 12-week-old female Wistar albino rats (48 for animal experiments, 4 for LC-MS analyses) weighing 200-250 g were used in this study. All procedures were approved by the Institutional Animal Care and Ethics Committee of Sivas Cumhuriyet University (Approval no: 567/2021). Rats with identical biological and physiological characteristics were purchased from organizations licensed to sell laboratory animals. Rat housing and *in vivo* experiments were conducted at the Animal Laboratory of the Faculty of Medicine, Sivas Cumhuriyet University. Animals were housed under standard conditions (22±2 ˚C, 12 hh light/dark cycle) with free access to food and water. The internationally accepted ARRIVE guideline 2.0 (Animal Research: Reporting of *ın vivo* Experiments) was applied from study design through publication of the results as a scientific article (18).

The number of animals was determined based on a power analysis (G*Power 3.1; effect size=0.4; α=0.05; power=0.8).

The rats were randomly divided into eight groups (n=6 per group) as shown in Table 1. The details of group treatments, drug dosages, and timing of ischemia/reperfusion procedures are summarized in Table 1.

1. Control group
2. MMF group
3. NF group
4. Ischemia (I) group
5. Ischemia-Reperfusion (I/R) group
6. I/R+MMF (30 mg/kg, i.p.) group
7. I/R+NF (5 mg/kg, i.p.) group
8. I/R+MMF+NF group

Ischemia was induced for 3 hr, followed by 24 hr of reperfusion, based on established protocols for ovarian torsion models (19). These durations represent the period sufficient to induce measurable oxidative and histological changes without irreversible necrosis.

Table 1. Research procedures and drugs applied to the rat study groups

Study groups (n=6)	Preop drug	1. laparotomy	Postoperative medicine	2. laparatomy
Control group	Saline 2.5 ml intraperitoneally (IP) was administered 30 min before the operation	Ovaries observed for 1 min	Saline 2.5 ml IP was administered at the 8th and 16th hr postoperatively	Bilateral oophorectomy was performed with the second laparotomy 24 hr after the first laparotomy
MMF group	MMF 10 mg/kg/2.5 ml was administered 30 min before the operation	Ovaries observed for 1 min	MMF 10 mg/kg/2.5 ml was administered at the 8th and 16th hr postoperatively	Bilateral oophorectomy was performed with the second laparotomy 24 hr after the first laparotomy
NF group	NF 20 mg/kg/2.5 ml IP was administered 30 min before the operation	Ovaries observed for 1 min	NF 20 mg/kg/2.5 ml IP was administered at the 8th and 16th hr postoperatively	Bilateral oophorectomy was performed with the second laparotomy 24 hr after the first laparotomy
Ischemia group	A single laparotomy was performed. Ischemia* was applied. At the end of the period, the rats were sacrificed, and bilateral oophorectomy was performed *Ischemia: After the bilateral ovaries were rotated 720 degrees clockwise together with the tubo-ovarian vessels, they were clamped with a pedicled bulldog clamp. The ischemia time was determined as 3 hr			
Ischemia/reperfusion (I/R) group	Ischemia followed by reperfusion** was performed **Reperfusion: At the end of the 3-hour ischemia period, the ovary was restored by opening the clamp			Bilateral oophorectomy was performed with the second laparotomy 24 hr after the first laparotomy
MMF-I/R group	Ischemia was applied MMF 10 mg/kg/2.5 mL IP was administered 30 min before reperfusion		MMF 10 mg/kg/2.5 ml was administered at the 8th and 16th hr postoperatively	Bilateral oophorectomy was performed with the second laparotomy 24 hr after the first laparotomy
NF-İR group	Ischemia was applied NF 20 mg/kg/2.5 mL IP was administered 30 min before reperfusion		NF 20 mg/kg/2.5 ml IP was administered at the 8th and 16th hr postoperatively	Bilateral oophorectomy was performed with the second laparotomy 24 hr after the first laparotomy
MMF-NF-İR group	Ischemia was applied MMF 10 mg/kg/2.5 mL and NF 20 mg/kg/2.5 ml IP were administered 30 min before reperfusion		Drug administrations were repeated after 8 and 16 hr	Bilateral oophorectomy was performed with the second laparotomy 24 hr after the first laparotomy

MMF: Monomethyl fumarate; NF: Nifedipine

First laparotomy procedure

After anesthesia with ketamine (50 mg/kg)+xylazine (10 mg/kg), a midline abdominal incision was made. In the ischemia and I/R groups, the right ovarian pedicle was rotated 360° clockwise and fixed with 5-0 silk suture to block blood flow. Successful ischemia was confirmed by the ovary's color change to a dark bluish tone. During ischemia, body temperature was maintained at 37 ˚C using a heating pad (20, 21).

Second laparotomy procedure

After 3 hr of ischemia, reperfusion was achieved by detorsion of the ovarian pedicle and restoration of blood flow. Color returning to normal pink confirmed successful reperfusion. Animals were kept under the same housing conditions during the 24 hr reperfusion period. At the end of reperfusion, blood samples were collected from the tail vein for hormonal and biochemical assays, and the animals were sacrificed by cervical dislocation under deep anesthesia. Ovarian tissues were quickly removed and divided for biochemical, histological, and molecular analyses (21, 22).

Sample collection process

All blood samples were collected at the end of the reperfusion period and centrifuged at 5000 rpm for 10 min at +4 ˚C. The serum was transferred into Eppendorf tubes and stored at -80 ˚C until biochemical and hormonal analyses. These samples were used to determine hormonal alterations caused by ovarian ischemia-reperfusion injury. During the second laparotomy, both ovaries were excised. One ovary was divided equally into two parts: one half fixed in 10% neutral-buffered formalin for 48 hr for histological and immunohistochemical (IHC) analysis, and the other half stored at -80 ˚C for biochemical assays. The second ovary was placed in RNAlater solution (Invitrogen, USA) to preserve RNA integrity for quantitative reverse-transcriptase real-time polymerase chain reaction (RT-qPCR) analysis and stored at -80 ˚C until RNA extraction. The quantification of drug-active compounds transferred to ovarian tissue was determined by LC-MS. For this purpose, rats (n=4) were sacrificed 6 hr after intraperitoneal administration of MMF (Sigma-Aldrich, Germany; 10 mg/kg in 2.5 ml) and NF (Sigma-Aldrich, Germany; 20 mg/kg in 2.5 ml). Ovarian tissues were excised, pretreated, and analyzed using a Shimadzu LC-MS-8045 triple quadrupole mass spectrometer. MMF and NF stock solutions were prepared at 1 mg/ml concentrations, and calibration standards were generated from serial dilutions to construct a standard curve. Quantification was based on the calibration curve using area-under-curve values specific to each compound (23).

Gene expression analysis (mRNA-qRT PCR method)

Total RNA was isolated using GeneAll Hybrid-R RNA Purification Kit (GeneAll, Korea). cDNA synthesis was performed with WizScript™ cDNA Synthesis Kit (High Capacity, W2211), and quantitative RT-qPCR with WizPure™ qPCR Master (SYBR, W1711) on an Applied Biosystems Real-Time PCR System (23). Primer sequences are listed in Table 2. Each reaction was run in duplicate. GAPDH was used as a housekeeping gene, and relative expression was calculated by the 2^−ΔΔCt method (24). The procedures followed **were** adapted from the β-cryptoxanthin ischemia/reperfusion model described by Mohammadnejad *et al.* (25).

Table 2. The primer sequences used for RT-qPCR in gene expression analysis are listed

Primer name	Primers (5'→3')
HIF-1 α -F	CCTGCAACTGAATCAAGAGGTTGC
HIF-1 α -R	CCATCAGAAGGACTTGCTGGCT
NFkB-F	GCAAACCTGGGAATACTTCATGTGACTAAG
NFkB-R	ATAGGCAAGGTCAGAATGCACCAGAAGTCC
Nrf2-F	CTCTCTGGAGACGGCCATGACT
Nrf2-R	CTGGGCTGGGGACAGTGGTAGT
KEAP1-F	TGGGCGTGGCAGTGCTCAAC
KEAP1-R	GCCCATCGTAGCCTCCTGCG
EPO-F	CTCCGAACAATCACTGCT
EPO-R	GGTCATCTGTCCCCTGTCCT
GLUT1-F	TGGCCAAGGACACACGAATACTGA
GLUT1-R	TGGAAGAGACAGGAATGGGCGAAT
PDK-F	CTCACAGAAGGGCCACATTT
PDK-R	AGCATCTGGACTGCTCTGGGT
SUMO-F	ATTGCCCTTCTTCCTTTA
SUMO-R	TTCCACAGTTCGGTTCTC
VEGF-F	CATCCACCATGCACTTGCTGT
VEGF-R	GGCTGCTCCAAACTCCTTCCA
MAPK14-F	CGAAATGACCGGCTACGTGG
MAPK14-R	CACTTCATCGTAGGTCAGGC
HO1-F	TCTATCGTGCTCGCATGAAC
HO1-R	CAGCTCCTCAAACAGCTCAA
HSP70-F	ACCTTCGACGTGTCCATCCTGA
HSP70-R	TCCTCCACGAAGTGGTTCACCA
HSP90-F	GCTTTCAGAGCTGTTGCGGTAC
HSP90-R	AAAGGCGGAGTTAGCAACCTGG
CAT-F	CCAGAAGCCTAAGAATGCAA
CAT-R	TCCCTTGGCAGCTATGTGAGA
GPX-F	GCTGTGCGCGCTCCAT
GPX -R	ACCATGTGCCCATCGATGT
SOD2-F	TAACGCGCAGATCATGCAGCTG
SOD2-R	AGGCTGAAGAGCGACCTGAGTT
ENOS-F	TACGGAGCAGCAAATCCAC
ENOS-R	GATCAAAGGACTGCAGCCTG
İNOS-F	ATGGAACAGTATAAGGCAAACACC
İNOS-R	GTTTCTGGTCGATGTCATGAGCAAAGG
GAPDH-F	AGAACATCATCCCTGCATCC
GAPDH-R	GTCCTCAGTGTAGCCCAGGA

Biochemical analyzes

Serum samples stored at -80 ˚C were thawed at room temperature before analysis. The samples were then centrifuged (Hettich Rotina 380R, Germany) at 3,000 rpm for 10 min at 4 ˚C to remove any residual particles. The resulting clear supernatants were carefully collected and used for subsequent biochemical analyses.

Lipid peroxidation levels were determined by measuring malondialdehyde (MDA) using a commercial Lipid Peroxidation (MDA) Assay Kit rer's instructions. Total oxidant status (TOS) was assessed using the Rel Assay Diag(Colorimetric/Fluorometric, ab118970, Abcam, UK) following the manufactu nostics Kit (Gaziantep, Turkey), and results were expressed in μmol H_2O_2 equivalent/L. To evaluate DNA oxidative damage, 8-hydroxy-2′-deoxyguanosine (8-OHdG) levels were measured in tissue homogenates using an ELISA kit (MyBioSource, USA, Cat. No. MBS263942). Total Advanced Oxidation Protein Products (AOPP), representing oxidative protein damage, were determined using the Rat AOPP ELISA Kit (MyBioSource, USA, Cat. No. MBS930313) according to the manufacturer's protocol. Serum anti-Müllerian hormone (AMH) and estradiol (E2) levels were measured using ELISA kits (MyBioSource, USA) to assess ovarian reserve and endocrine function after I/R injury. These parameters collectively reflect oxidative damage to lipids, proteins, and DNA, as well as ovarian functional impairment following ischemia-reperfusion (26-28).

Light microscopic experiments

After the experiments, all ovarian tissues were fixed in 10% neutral-buffered formalin for 48 hr. Tissue processing was performed using a Leica TP1020 tissue processor (Germany) according to standard histological protocols. After dehydration, tissues were embedded in paraffin, and 4-5 μm sections were cut using a Leica RM2235 microtome (Germany). Following deparaffinization, the sections were rehydrated through a series of ethanol dilutions and rinsed in distilled water. Subsequently, the sections were prepared for hematoxylin–eosin (H&E) staining, immunofluorescence staining, and TUNEL assay.

Hematoxylin–eosin (H&E) staining

Sections were immersed in Mayer's hematoxylin solution (Bio-Optica, Milano, Italy) for 10 min for nuclear staining, rinsed in running tap water, and briefly differentiated with acid alcohol. After bluing in ammonia water, they were counterstained with eosin (Bio-Optica, Milan, Italy) for 4 min. Tissues were dehydrated in graded ethanol series and cleared in three changes of xylene before mounting with Entellan (Merck, Darmstadt, Germany). Stained sections were examined under a light microscope (Olympus BX53, Japan). Histopathological damage, including hemorrhage, follicular degeneration, interstitial edema, and vascular congestion, was semi-quantitatively scored as follows: 0=no damage, 1=mild, 2=moderate, 3=severe (5, 29).

Immunofluorescence analysis

For immunofluorescence, sections were subjected to antigen retrieval by microwave heating in citrate buffer (pH 6.0) for 10 min, then cooled to room temperature. Tissue borders were outlined with a PAP pen, and sections were permeabilized in PBS containing 0.1% Triton X-100. To block nonspecific binding, slides were incubated in SuperBlock (Sky Tech Lab, USA) for 30 min at room temperature. Primary antibodies were applied and incubated overnight at 4 ˚C in a humidified dark chamber:

• Mouse monoclonal anti-8-OHdG (15A3, 1:100, Santa Cruz Biotechnology, sc-66036, California, USA)
• Rabbit polyclonal anti-4-Hydroxynonenal (1:100, Abcam, ab46545, Cambridge, UK)
• Rabbit polyclonal anti-Caspase-3 (NeoMarkers, Fremont, CA, USA)

After PBS rinsing, secondary antibodies were applied for 60 min at room temperature in the dark:

• Goat anti-rabbit IgG H&L (Alexa Fluor 488, ab150077, Abcam, UK) for Caspase-3 and 4-HNE (23)
• Goat anti-mouse IgG H&L (Alexa Fluor 568, ab175473, Abcam, UK) for 8-OHdG.

Nuclei were counterstained with DAPI (4′,6-diamidino-2-phenylindole, Sigma, USA) and coverslipped with antifade mounting medium suitable for fluorescence microscopy. Slides were examined using a fluorescence microscope (Olympus BX51, Japan). Immunoreactivity was semi-quantitatively scored according to fluorescence intensity: 0=no staining, 1=weak, 2=moderate, 3=strong staining (modified from immunofluorescence protocols described by Oberhaus and applied in ovarian ischemia/reperfusion models by Ulusoy Tangul *et al.* (30, 31)).

TUNEL assay

DNA fragmentation due to apoptosis was detected using the In Situ Cell Death Detection Kit (REF 1168795910, Roche, Germany) according to the manufacturer's instructions. Sections were rinsed in PBS (Sigma, USA) and treated with DNase I (Sigma, USA; 3000 U/ml–3 U/ml, 50 mM Tris/HCl, pH 7.5, 1 mg/mL BSA) for 10 min at 20±5 ˚C as a positive control for DNA cleavage. After PBS washes, 50 μl of TUNEL reaction mixture was applied to each section and incubated for 60 min at 37 ˚C in a dark, humid chamber. Slides were rinsed again in PBS and mounted with antifade medium. TUNEL-positive cells were visualized under a fluorescence microscope (Olympus BX51, Japan) using filters with excitation wavelengths of 450-500 nm.

Apoptotic index was calculated as the ratio of TUNEL-positive nuclei to total nuclei in ten randomly selected fields, in accordance with the combined TUNEL–immunofluorescence double-labeling procedure established by Oberhaus and adapted for ovarian I/R models by Ulusoy Tangul *et al.* (30-32).

LC-MS analysis

The quantification of MMF and NF concentrations in ovarian tissues was performed using a high-performance LC-MS system (Agilent 1260 Infinity II, USA). The system was equipped with a G7114A 1260DAD detector, G7311B 1260 Quad Pump system, G1328C manual injection unit, and G6125B LC/MSD detector for both chromatographic and mass detection. Chromatographic separation was achieved using an ACE C18 column (3 μm particle size, 100 Å pore size). The column temperature was maintained at 25 ˚C, and the mobile phase consisted of an acetonitrile–water (80:20, v/v) mixture delivered at a flow rate of 0.6 ml/min. The injection volume was 20 μl, and the UV detector wavelength was set at 254 nm. Ovarian tissues obtained from rats (n=4) six hours after intraperitoneal administration of MMF (10 mg/kg) and NF (20 mg/kg) were homogenized and extracted for LC–MS analysis. Samples were prepared in triplicate, filtered through 0.22 μm syringe filters, and injected directly into the LC-MS system. Quantification was performed using calibration curves generated from standard MMF and NF solutions prepared at 0.01-10 μg/ml. The concentration of each

compound in the tissue was calculated from the area under the curve (AUC) of the corresponding UV chromatogram. Instrument validation parameters (retention time, linearity, recovery, and reproducibility) were established before analysis to ensure quantification accuracy. The retention times for MMF and NF were 3.25±0.05 min and 4.02±0.07 min, respectively. All measurements were performed under controlled temperature and humidity conditions to minimize variability. These LC–MS procedures were adapted from validated bioanalytical protocols for MMF and NF in biological matrices and aligned with current guideline expectations (14).

Calibration curve

Stock solutions of MMF and NF were freshly prepared in methanol at a concentration of 1 mg/mL. Each compound was then serially diluted to obtain standard working solutions at concentrations of 0.01, 0.05, 0.1, 0.5, 1, 5, and 10 µg/mL. Twenty microliters of each concentration were injected into the LC–MS system under identical chromatographic conditions. Calibration curves were constructed by plotting the peak area (area under the curve, AUC) versus the corresponding concentration for each analyte. Both MMF and NF showed excellent linearity within the tested range, with correlation coefficients (R^2) greater than 0.998. The limit of detection (LOD) and limit of quantification (LOQ) were calculated using the signal-to-noise ratios of 3:1 and 10:1, respectively. The calibration data for MMF and NF are summarized in Table S.1, and the corresponding chromatograms are presented in Figure S.1 and Figure S.2. All calibration and validation procedures were performed following previously published LC–MS quantification studies in biological matrices (14, 33).

Pretreatment of ovarian tissues

After the ovarian tissue samples were thawed at room temperature, each specimen was weighed precisely (±0.001 g) and placed in 1.5 ml of 0.25 M sucrose solution. All tissues were homogenized using a mechanical tissue homogenizer (IKA T25 Ultra-Turrax, Germany) until a uniform suspension was obtained. An equal volume of dichloromethane (DCM) was added to each homogenate for solvent extraction. The mixture was vortexed and incubated for 10 min at room temperature to allow complete extraction of lipophilic compounds. To separate the organic and aqueous phases, samples were centrifuged at 15,000 rpm for 15 min at +4 ˚C. The extraction procedure was repeated three times per sample to maximize recovery efficiency. The combined organic phases were collected, evaporated under a gentle stream of nitrogen gas, and the residues were stored at 2-8 ˚C until LC-MS analysis. This protocol was optimized based on previously validated solvent-extraction procedures for drug quantification in biological tissues (14, 33).

Statistical analysis

All experimental data were expressed as mean±standard deviation (SD).

Statistical analysis was performed using GraphPad Prism version 10.0 (GraphPad Software, San Diego, CA, USA). Data were first evaluated for normality (Shapiro–Wilk test) and homogeneity of variances (Levene's test). Group differences were analyzed using one-way analysis of variance (ANOVA) followed by Welch and Brown–Forsythe post hoc tests to adjust for unequal variances when necessary. A P-value<0.05 was considered statistically significant. All graphs and tables were created using GraphPad Prism, and statistical significance (P<0.05, P<0.01, P<0.001) was reported consistently throughout the manuscript.

Results

RT-qPCR and ELISA experiments

The relative mRNA expression levels of HIF-1α, Nrf2, NF-κB, and associated oxidative-stress–related genes (EPO, GLUT1, PDK1, SUMO1, VEGF, MAPK14, HO-1, HSP70, HSP90, CAT, GPx, SOD2, eNOS, and iNOS) are presented as a heat-map in Figure 1. Gene expression was

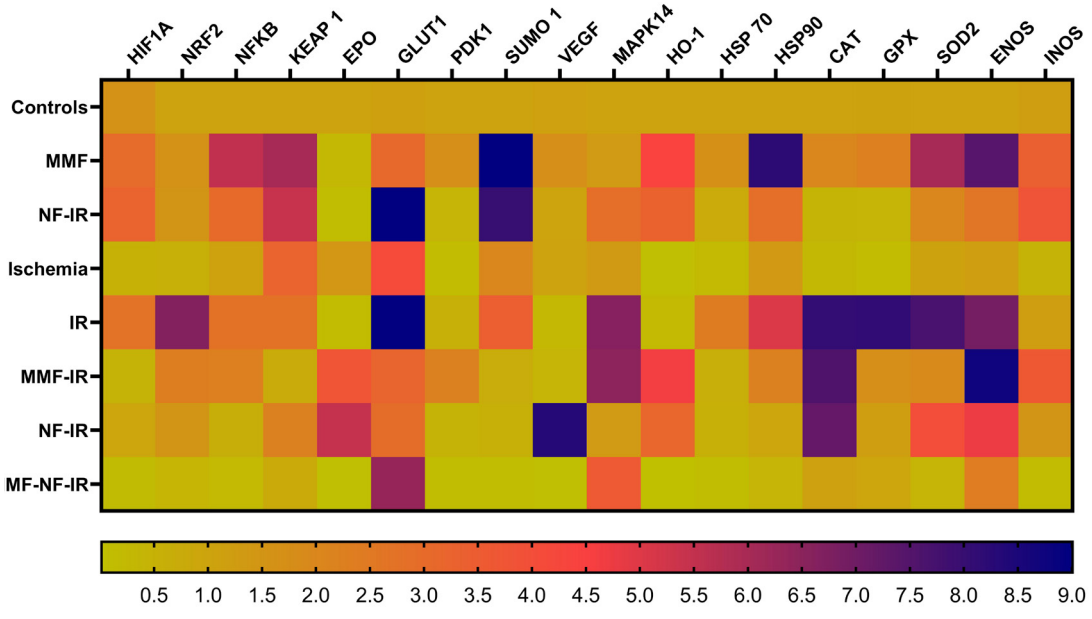

Figure 1. Heat map plot of the expression multiples of the genes studied in the rat study group
Expression multiples are presented as 0.5 and multiples. It shows that expression decreases up to values below 0.5 and increases up to 9 times

significantly upregulated in the ischemia-reperfusion (I/R) group compared to the ischemia-only group (P<0.05). Combined treatment with MMF+NF effectively normalized transcription factor and downstream gene expression, approaching levels observed in the control group (P>0.05).

Serum hormone profiles (AMH and E2) are summarized in Figure 2. AMH concentrations increased significantly following NF treatment during ischemia (P<0.05), whereas MMF administration during I/R resulted in AMH levels comparable to controls (P>0.05). Combined MMF+NF pretreatment before I/R did not differ significantly from the I/R group (P>0.05). In contrast, E2 levels decreased significantly after NF administration during ischemia (P<0.05), while MMF treatment produced a modest, non-significant decline (P>0.05). I/R itself caused a mild, non-significant elevation in serum E2 (P>0.05). NF pretreatment before I/R markedly reduced E2 compared to untreated I/R rats (P<0.05), whereas MMF and MMF + NF pretreatments showed no significant difference (P>0.05).

Oxidative stress–related biochemical parameters (TOS, MDA, 8-OHdG, and AOPP) are shown in Figure 3. Ischemia and I/R significantly increased serum TOS and MDA levels compared with controls (P<0.05). Both MMF and NF treatments reduced these elevations, although reductions were significant only in the combined MMF+NF group (P<0.05). Tissue 8-OHdG levels were also elevated after I/R, indicating oxidative DNA damage; however, MMF and NF monotherapies partially reduced these values, and MMF+NF pretreatment restored them to near baseline levels (P<0.05). Serum AOPP concentrations increased after MMF alone (P<0.05) but decreased significantly following NF treatment and after ischemia (P<0.05). Combined MMF+NF administration before reperfusion yielded a non-significant improvement compared to the I/R group (P>0.05).

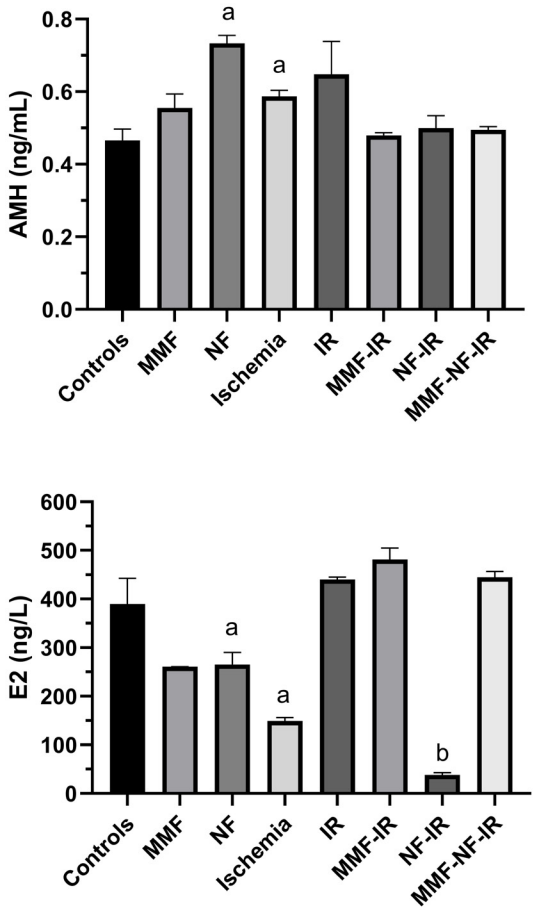

Figure 2. Rat serum hormone profile (anti-müllerian hormone and estradiol) levels
Data expressed as mean with SD. A denotes P<0.05 vs. controls and b denotes P<0.05 vs. IR
MMF: Monomethyl fumarate; NF: Nifedipine

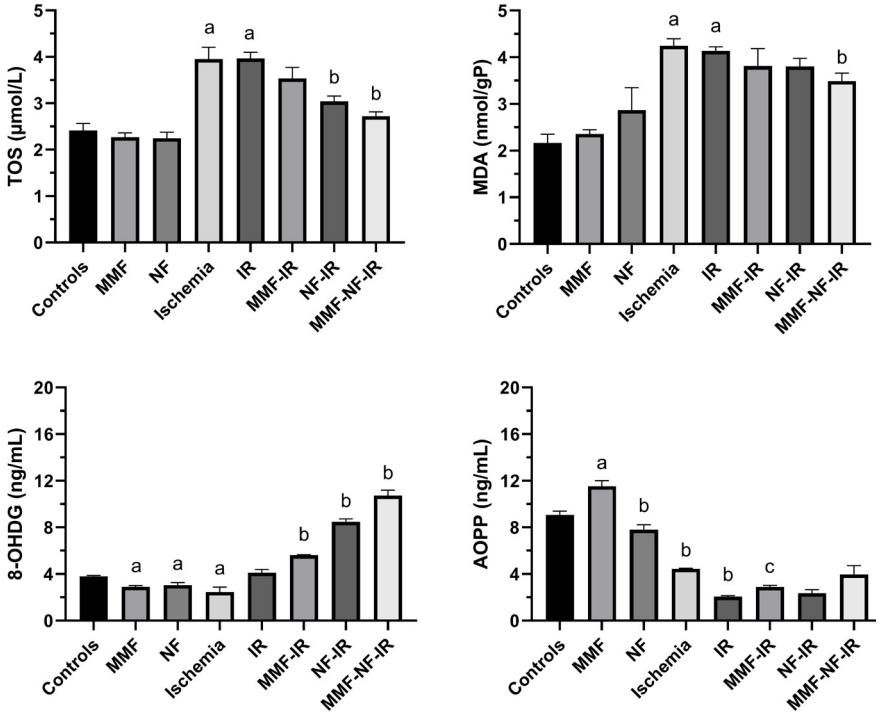

Figure 3. The serum TOS, MDA, 8-OHdG and AOPP levels measured by ELISA in rat study groups
The data are expressed as mean with SD. For the TOS, MDA, and 8-OHdG data, A denotes P<0.05 vs. controls and b denotes P<0.05 vs. IR. For the AOPP data, a and b denotes p&l
TOS: Total oxidant status, MDA: Malondialdehyde, AOPP: Advanced oxidation protein products, 8-OHdG: 8-hydroxydeoxyguanosine

Figure 4 illustrates the relative tissue protein levels of BAX, BECLIN-1, HIF-1α, Nrf2, and NF-κB. Pro-apoptotic BAX and autophagy-related BECLIN-1 levels increased significantly after ischemia (P<0.05). They were reduced by MMF and NF treatments, with the most pronounced decrease observed in the combined group (P<0.01). HIF-1α expression was markedly upregulated in I/R (P<0.05), while MMF+NF treatment reduced it to near-control values (P<0.05). Nrf2 expression followed a similar pattern, showing activation during I/R (P<0.05) and normalization after combined therapy (P<0.05 vs I/R). NF-κB activation paralleled HIF-1α and Nrf2 trends, supporting the modulatory effects of MMF and NF on oxidative stress–responsive transcription factors.

Overall, MMF and NF—particularly in combination—attenuated ischemia-reperfusion–induced oxidative stress and apoptosis, preserved hormonal balance, and normalized transcription-factor expression. These findings were statistically validated using one-way ANOVA, followed by Welch and Brown-Forsythe *post hoc* tests, with significance set at P<0.05.

Histological and IHC findings

H&E–stained ovarian sections from the control, MMF, and NF groups displayed a normal histological appearance. The germinal epithelium was intact with cuboidal organization and a well-preserved basement membrane. Primordial, primary, secondary, and tertiary follicles exhibited normal morphology with regularly arranged granulosa cells and intact zona pellucida. The cortex and medulla contained normal connective tissue, and vascular structures were of typical number and appearance (Figure 5; 1-3).

In contrast, the ischemia and I/R groups exhibited pronounced histopathological alterations, including disruption of the germinal epithelium, follicular degeneration, disorganization of granulosa cells, and loss of zona pellucida integrity. Severe hemorrhage, interstitial edema, and mononuclear inflammatory cell infiltration were observed in the cortical and medullary connective tissues (Figure 5; 4, 5). In the I/R+MMF and I/R+NF groups, partial recovery of follicular structure was evident. Follicular organization and zona pellucida morphology

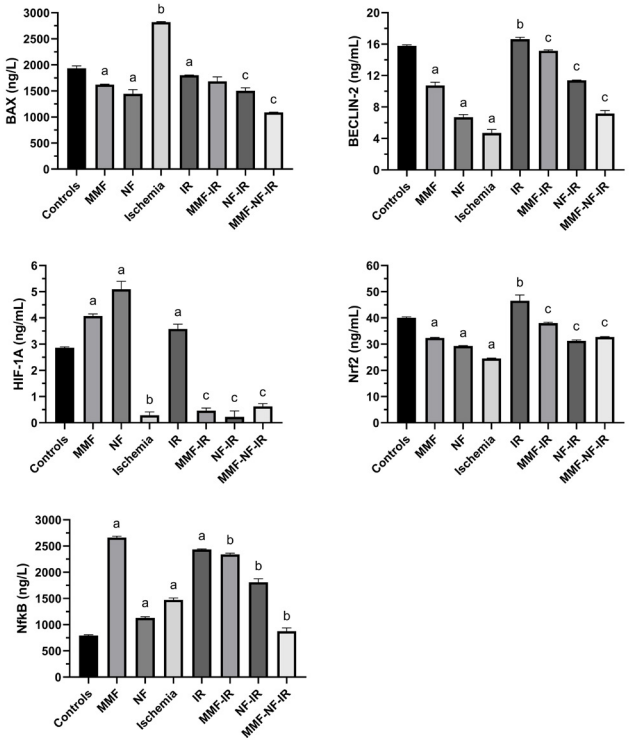

Figure 4. Tissue of rat avary BAX, BECLIN-2, HIF-1a, Nrf2, and NfkB levels measured by ELISA
The data are expressed as mean with SD. For the BAX, BECLIN-2, HIF-1a, and Nrf2 data, a and b denotes P<0.05 vs. controls and c denotes P<0.05 vs IR. For the NfkB HIF1a: Hypoxia-inducible factor-1a, NRF2: Nuclear factor erythroid 2-related factor 2, NfkB: Nuclear Factor kappa B

were notably improved compared to the I/R group, with reduced hemorrhage and inflammatory infiltration (Figure 5; 6, 7). The I/R+MMF+NF group exhibited near-normal morphology, comparable to that of the control group (Figures 5 and 8). Semi-quantitative histopathological scoring (0-3) revealed significantly higher damage scores in the ischemia and I/R groups than controls (P<0.01), whereas MMF and NF monotherapies reduced tissue injury (P<0.05), and the combined MMF+NF group showed the most significant protection (P<0.001; Table 3).

Caspase-3 immunoreactivity was markedly elevated in the ischemia and I/R groups compared to controls (P<0.01),

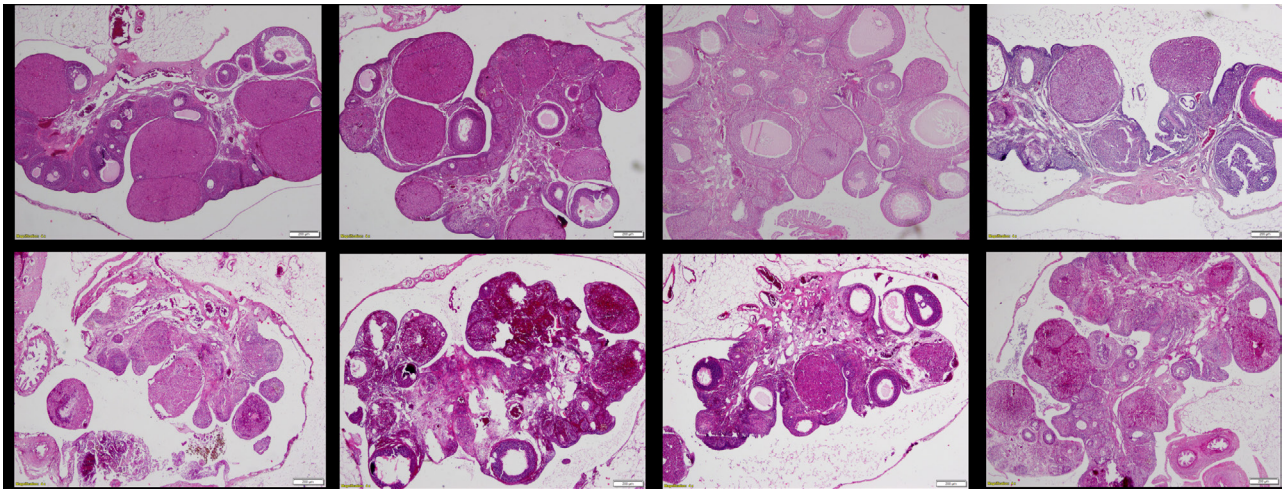

Figure 5. Hematoxylin-eosin stained sections of rat ovaries

Table 3. Quantification of monomethyl fumarate (MMF) and nifedipine (NF) in rat ovarian tissues

No	MMF	Amount of MMF (mg)	NF	Amount of NF (mg)
1	MMF1	0,031	NF1	0,020
2	MMF2	0,024	NF2	0,026
3	MMF3	0,025	NF3	0,023
4	MMF4	0,032	NF4	0,024

MMF: Monomethyl fumarate; NF: Nifedipine

confirming apoptotic activation (Figure 6; 1, 2). Treatment with MMF and NF significantly reduced Caspase-3 staining intensity, with the lowest signal in the I/R+MMF+NF group (P<0.001; Figure 6; 3-6).

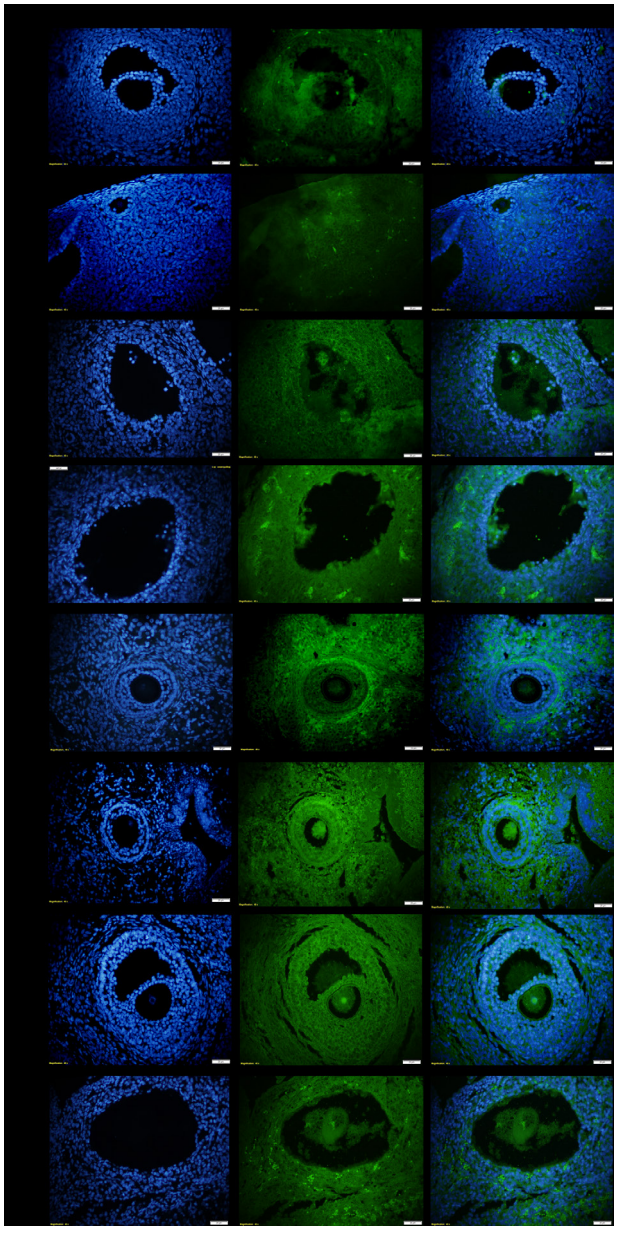

Figure 6. Green color visualization of Caspase 3 antibody in ovarian tissue with Goat Anti-Rabbit IgG H&L (Alexa Fluor® 488) secondary antibody by immunofluorescence method. Blue fluorescent images of cell nuclei with DAPI staining and the rat imag
DAPI: 4′,6-diamidino-2-phenylindole, Sigma, USA

4-Hydroxynonenal (4-HNE) staining, indicative of lipid peroxidation, was also significantly higher in the ischemia and I/R groups than in controls (P<0.01). No difference was detected among the control, MMF, and NF monotherapy groups (P>0.05). However, both I/R+MMF and I/R+NF treatments reduced 4-HNE positivity, and the I/R+MMF+NF group demonstrated the lowest immunoreactivity (P<0.001; Figure 7).

8-OHdG immunoreactivity, reflecting oxidative DNA damage, increased significantly in the ischemia and I/R groups compared to the control (P<0.01; Figure 8; 1, 2). MMF and NF monotherapies attenuated this elevation (P<0.05), and the combined MMF+NF group showed a near-complete normalization of 8-OHdG staining intensity (P<0.001; Figure 8; 3-5). TUNEL assay results are illustrated in Figure 9. Apoptotic nuclei were abundant in the ischemia and I/R groups, whereas the control, MMF, and NF groups displayed minimal apoptosis. Quantitative analysis

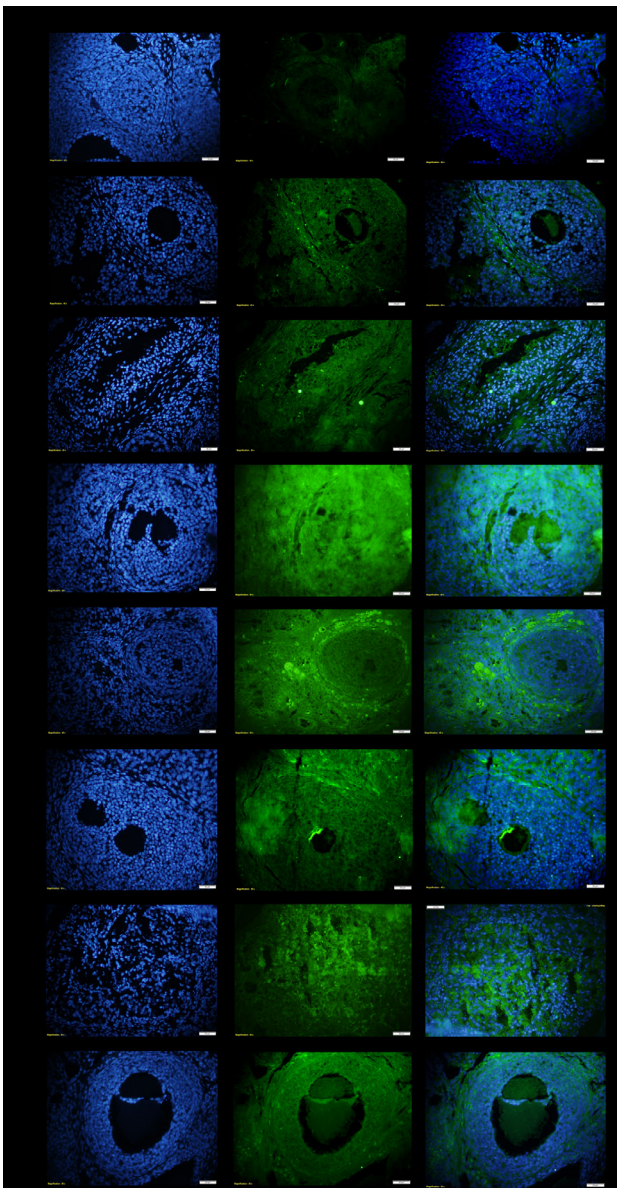

Figure 7. Anti-4 Hydroxynonenal antibody in ovarian tissue with immunofluorescence method and Goat Anti-Rabbit IgG H&L (Alexa Fluor® 488) secondary antibody in green color. Blue fluorescent images of cell nuclei with DAPI staining and the rat image
DAPI: 4′,6-diamidino-2-phenylindole, Sigma, USA

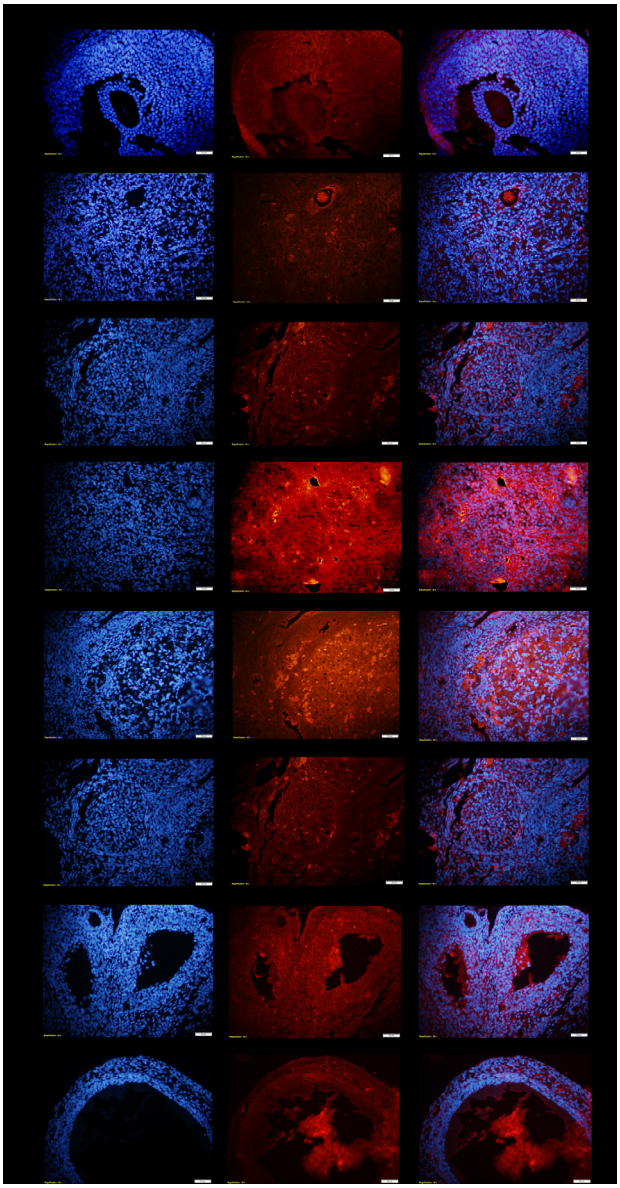

Figure 8. The appearance of 8-OHdG antibody in rat ovary tissue in red with Goat Anti-Mouse IgG H&L (Alexa Fluor® 568) secondary antibody by immunofluorescence method. Blue fluorescent images of cell nuclei with DAPI staining and the image obtaine
DAPI: 4′,6-diamidino-2-phenylindole, Sigma, USA

of TUNEL-positive cell counts confirmed a significant reduction in apoptosis in I/R+MMF (P<0.05), I/R+NF (P<0.01), and I/R+MMF+NF (P<0.001) groups compared to I/R alone (Figure 9; 6). In summary, histological and IHC evaluations demonstrated that MMF and NF, particularly when used in combination, preserved ovarian tissue integrity, decreased oxidative and apoptotic markers, and significantly mitigated ischemia–reperfusion–induced injury.

LC-MS results

LC-MS analysis confirmed the detection and quantification of MMF and NF within ovarian tissues following intraperitoneal administration. After dichloromethane (DCM) extraction and solvent evaporation, each dried tissue sample was reconstituted in 200 µl methanol, vortexed, and centrifuged at 3000 rpm for 10 min at +4 ˚C. The resulting supernatant was injected into the LC-MS system under the chromatographic conditions defined in Section 2.5. Quantification was based on calibration curves generated in Section 2.5.1 (R^2>0.998). The retention times for MMF and NF were 3.25±0.05 min and 4.02±0.07 min, respectively. Representative chromatograms and peak integration profiles are shown in Figure 10, while Table 3 summarizes individual drug quantities measured in rat ovarian tissues.

No MMF or NF peaks were detected in the control or I/R groups, confirming analytical specificity. Extraction recoveries exceeded 93%, validating the accuracy and reproducibility of the LC-MS protocol. These findings confirm that both compounds effectively penetrated ovarian tissue and were quantifiable within physiological ranges, supporting the pharmacological validity of the experimental design. Quantification accuracy and reproducibility were ensured by validating linearity, recovery, and retention parameters before analysis. These LC-MS procedures were adapted from previously validated bioanalytical protocols for fumarate derivatives and calcium channel blockers in biological matrices (14, 33).

Discussion

The present study was designed to evaluate the biochemical, histological, and molecular effects of MMF and NF in an experimentally induced rat model of ovarian

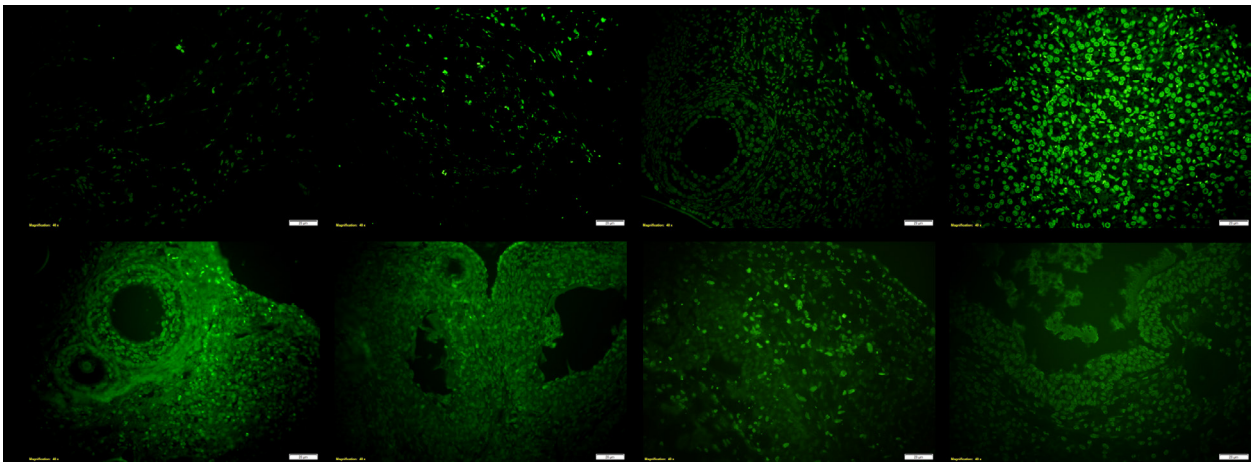

Figure 9. Green fluorescence image of apoptotic cells in rat ovary tissues by TUNEL staining
(1) Control group, (2) MMF group, (3) NF group, (4) Ischemia group, (5) IR group, (6) IR+MMF group, (7) IR+NF group, and (8) IR +MMF+NF group
MMF: Monomethyl fumarate; NF: Nifedipine

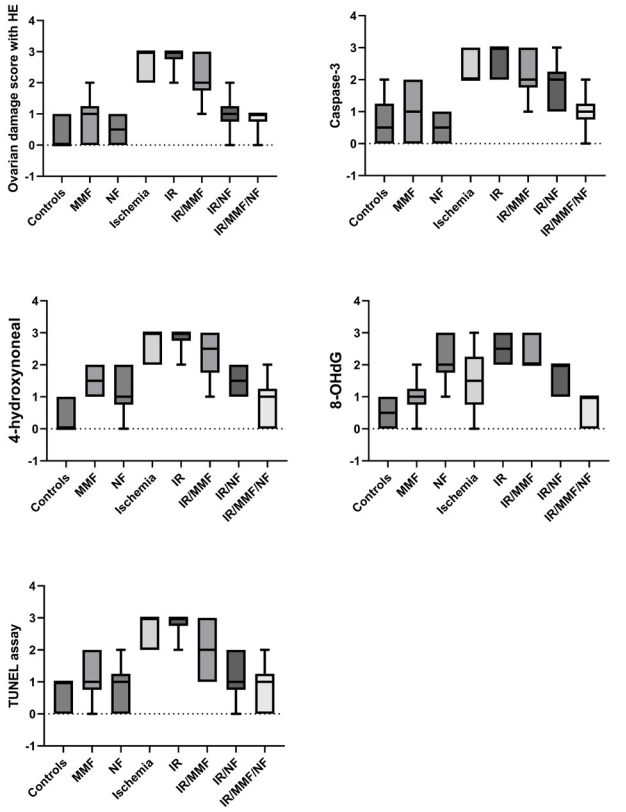

Figure 10. Ovarian damage score with hematoxylin-eosin (HE) and immunohistochemical evaluation results with caspase-3, 4-hydroxynoneal, 8-OHdG and TUNEL assay in study groups
Data are presented as box and whisker graphics

I/R. Before interpreting the biochemical and molecular findings, it is essential to consider the methodological framework, since the reliability of our conclusions depends on the precision of ischemia and reperfusion induction. Our dual-laparotomy design, consisting of a first laparotomy for ischemia induction and a second laparotomy for tissue and blood collection, was based on validated ovarian torsion–detorsion protocols. The ischemia period of 3 hr, followed by 24 hr of reperfusion, was optimized to elicit reproducible oxidative and apoptotic responses without inducing irreversible necrosis. This design was adapted and modified from Kalyoncu *et al.* and Ulusoy Tangul *et al.*, both of which employed similar ischemia–reperfusion durations and sampling intervals to assess pharmacological interventions in ovarian tissue (31, 34). Temperature control, anesthesia type, and tissue-handling steps were standardized according to these models. Furthermore, inclusion of LC-MS-based quantification of MMF and NF in ovarian tissues represents a methodological advancement, enabling the correlation of pharmacokinetic parameters with molecular and histological outcomes. Together, these refinements confirm that our experimental setup provides a physiologically relevant and reproducible model for evaluating antioxidant, inflammatory, and apoptotic responses after ovarian I/R injury (35).

Ovarian I/R injury in our model caused significant activation of oxidative stress–responsive transcription factors, including HIF-1α, NF-κB, and Nrf2, which collectively modulate redox homeostasis and apoptosis (36, 37). The combined administration of MMF and NF markedly attenuated these alterations, restoring gene expression levels to near control levels and demonstrating synergistic antioxidant and cytoprotective effects. Similar regulatory cross-talk among HIF-1α, NF-κB, and Nrf2 in I/R injury has been documented by Zhang *et al.*, supporting our findings that coordinated modulation of these pathways enhances cellular adaptation to oxidative stress (38). Histological analyses corroborated the molecular results: Severe hemorrhage, edema, and follicular degeneration observed in ischemia and I/R groups were markedly reduced in the MMF+NF group, which exhibited nearly normal ovarian morphology. Immunofluorescence and TUNEL analyses revealed decreased caspase-3, 4-hydroxynonenal (4-HNE), and 8-OHdG immunoreactivities, confirming suppression of lipid peroxidation, DNA oxidation, and apoptosis. These results are consistent with recent studies using antioxidant compounds such as silymarin and bromelain, which have also shown decreased oxidative and apoptotic indices in ovarian I/R models (31, 39).

Mechanistically, activation of the Nrf2/HO-1 pathway appears to be a key determinant of the observed protection. Dimethyl fumarate (DMF), the parent compound of MMF, was shown by Qi *et al.* to protect hepatic tissue against I/R injury by activating the NRF2/SLC7A11/HO-1 axis and suppressing ferroptosis, a mechanism consistent with our data (40). In parallel, calcium-channel blockade by NF can inhibit mitochondrial calcium overload and ROS production, thereby reducing NF-κB activation and apoptosis. This mechanism aligns with the findings of Manohar *et al.*, who demonstrated that NF decreases hypoxia-induced cell death via mitochondrial modulation (16). Together, these data support the conclusion that MMF and NF act through complementary mechanisms—MMF by promoting antioxidant defense via Nrf2, and NF by limiting calcium-dependent ROS generation and NF-κB signaling.

Minor discrepancies between oxidative DNA (8-OHdG) and protein (AOPP) levels in our results may reflect temporal differences in the onset of molecular damage, since DNA oxidation peaks earlier during reperfusion than protein oxidation. This temporal pattern is consistent with observations by Kalyoncu *et al.* and Öztürk *et al.*, who reported phase-dependent changes in DNA and protein oxidation despite overall reduction in oxidative stress (34,39). Histopathologically, our data showed connective tissue deposition and partial follicular depletion after I/R, which correspond to fibrosis-like remodeling processes also described by Kula *et al.* (41). The marked reduction in TUNEL-positive cells and caspase-3 immunoreactivity in the combined-therapy group further underscores the efficacy of MMF+NF in preserving follicular integrity and limiting apoptotic progression.

In summary, this study provides evidence that MMF and NF, when administered together, exert synergistic protective effects against ovarian ischemia–reperfusion injury through coordinated modulation of HIF-1α, NF-κB, and Nrf2 pathways. The methodological robustness of the dual-laparotomy design, validated ischemia/reperfusion durations, and LC–MS confirmation of tissue drug levels strengthen the translational value of the findings. These results highlight the combined activation of Nrf2-dependent antioxidant defense and inhibition of NF-κB/HIF-1α signaling as a promising therapeutic strategy for oxidative tissue injury in ovarian I/R and related reproductive ischemic pathologies.

Conclusion

This study identifies MMF and NF as promising agents for protecting ovarian tissue against I/R-induced injury by modulating the HIF-1α/NF-κB/Nrf2 signaling network and suppressing oxidative stress, apoptosis, and autophagy. The combination therapy demonstrated synergistic efficacy, restoring hormonal balance (AMH and E2), improving histological morphology, and reducing biochemical markers of oxidative stress. These findings provide mechanistic insight into the cross-talk between redox-responsive transcription factors and support the translational potential of MMF and NF for fertility-preserving strategies in ovarian torsion. Future studies are warranted to explore long-term reproductive outcomes and dose-response optimization.

Acknowledgment

This project was supported by the TÜBİTAK 1002 rapid support project, numbered 221S041, and the Cumhuriyet University Scientific Research Projects (CUBAP) with number T-2021-936.

Authors' Contributions

B K and A C provided the study design. B K, A C, and ZDS I collected the data. B K and A C performed the statistical analysis. B K, ZDS I, SD D, and GP C interpreted the data. B K, A C, ZDS I, SD D, and GP C prepared the manuscript. B K, A C, and ZDS I conducted the literature search. BK collected the funds.

Conflicts of Interest

The authors declare there are no conflicts of interest.

Declaration

We have not used any AI tools or technologies to prepare this manuscript.

References

1. Cowled P, Fitridge R. Pathophysiology of Reperfusion Injury. In: Fitridge R, Thompson M, editors. Mechanisms of Vascular Disease: A Reference Book for Vascular Specialists. Adelaide (AU): University of Adelaide Press; 2011. 18.
2. Huang C, Hong MK, Ding, DC. A review of ovary torsion. Tzu Chi Med J 2017; 29: 143–147.
3. Gupta A, Gadipudi A, Nayak D. A five-year review of ovarian torsion cases: Lessons learnt. J Obstet Gynaecol India 2020; 70: 220-224.
4. Soleimanzadeh A, Kian M, Moradi S, Mahmoudi S. Carob (*Ceratonia siliqua* L.) fruit hydro-alcoholic extract alleviates reproductive toxicity of lead in male mice: Evidence on sperm parameters, sex hormones, oxidative stress biomarkers and expression of *Nrf2* and *iNOS*. Avicenna J Phytomed 2020; 10: 35-49.
5. Gulakar B, Sebin SO, Laloglu E, Tanyeli A, Güler MC, Erbas E, *et al*. New potential agent in ovarian ischemia reperfusion injury: Alpha pinene. Journal of Biochemical and Molecular Toxicology, 39(6), e70318.
6. Fede MS, Daziani G, Tavoletta F, Montana A, Compagnucci P, Goteri G, *et al*. Myocardial ischemia/reperfusion injury: Molecular insights, forensic perspectives, and therapeutic horizons. Cells 14: 1509.
7. Zheng J, Chen P, Zhong J, Cheng Y, Chen H, He Y, Chen C. HIF-1α in myocardial ischemia-reperfusion injury (Review). Mol Med Rep 2021; 23: 352.
8. Heck-Swain KL, Koeppen M. The intriguing role of hypoxia-inducible factor in myocardial ischemia and reperfusion: A comprehensive review. J Cardiovasc Dev Dis 2023; 10: 215.
9. Mostahsan Z, Azizi S, Soleimanzadeh A, Shalizar-Jalali A. The protective roles of Mito-TEMPO on testicular ischemia-reperfusion injury based on biochemical and histopathological evidences in mice. Iran J Vet Surg 2024; 19: 97-105.
10. Lin PY, Stern A, Peng HH, Chen JH, Yang HCh. Redox and metabolic regulation of intestinal barrier function and associated disorders. Int J Mol Sci 2022; 23: 14463.
11. Asma ST, Acaroz U, Imre K, Morar A, Shah SRA, Hussain SZ, *et al*. Natural products/bioactive compounds as a source of anticancer drugs. Cancers (Basel) 2022; 14: 6203.
12. Yuan L, Wang Y, Li N, Yang X, Sun X, Tian H, *et al*. Mechanism of action and therapeutic implications of Nrf2/HO-1 in inflammatory bowel disease. Antioxidants 2024; 13: 1012.
13. Kabirian A, Batavani RA, Asri-Rezaei S, Soleimanzadeh A. Comparative study of the protective effects of chicken embryo amniotic fluid, vitamin C and coenzyme Q10 on cyclophosphamide-induced oxidative stress in mice ovaries. Vet Res Forum 2018; 9: 217-224.
14. Avery TD, Liu J, Loh DJLT, Abell AD, Grace PM, Li J, *et al*. Site-specific drug release of monomethyl fumarate to treat oxidative-stress disorders. Nat Biotechnol 2025; 43: 1624-1627.
15. Soleimanzadeh A, Kian M, Moradi S, Malekifard F. Protective effects of hydro-alcoholic extract of Quercus brantii against lead-induced oxidative stress in the reproductive system of male mice. Avicenna J Phytomed 2018; 8: 448-456.
16. Manohar K, Gupta RK, Gupta P, Saha D, Gare S, Sarkar R, *et al*. FDA-approved L-type channel blocker nifedipine reduces cell death in hypoxic A549 cells through modulation of mitochondrial calcium and superoxide generation. Free Radic Biol Med 2021; 177: 189-200.
17. Mostahsan Z, Azizi S, Soleimanzadeh A, Shalizar-Jalali A. Protective effects of Mito-TEMPO on ischemia-reperfusion injury in a mouse testicular torsion and detorsion model. Vet Res Forum 2024; 15: 665-672.
18.Percie du Sert N, Hurst V, Ahluwalia A, Alam S, Avey MT, Baker M, *et al*. The ARRIVE guidelines 2.0: Updated guidelines for reporting animal research. Br J Pharmacol 2020; 177: 3617-3624.
19. Kalkan İ, Turan S, Demir A, Ergin A. The molecular mechanism of the protective effect of tianeptine against ovarian ischemia–reperfusion injury. Sci Rep 2025; 15: 28141.
20. Arslan S, Aşır F, Özkorkmaz EG, Azizoğlu M, Basuguy E, Okur MH, *et al*. Protective effects of passiflora incarnata on ovarian ischemia/reperfusion damage in rats with ovarian torsion. Ulus Travma Acil Cerrahi Derg 2023; 29: 1344-1350.
21. Sezgin A, Emniyet Sert AA, Take Kaplanoğlu G, Karakaya C, Demirdağ E, Cevher Akdulum MF, *et al*. Assessing the potential of nifedipine and resveratrol to enhance ovarian viability in conjunction with detorsion treatment: A rat ovarian torsion model study. Turk J Obstet Gynecol 2025; 22: 154-162.
22. Bulutlar E, Bozdağ H, Yılmaz A, Ulutku Bulutlar GB, Çoban Ramazan D. Healing effect of genistein on detorsioned rats after experimental ovarian torsion. South Clin Ist Euras 2025; 36: 155-159.
23. Baqerkhani M, Soleimanzadeh A, Mohammadi R. Effects of intratesticular injection of hypertonic mannitol and saline on the quality of donkey sperm, indicators of oxidative stress, and testicular tissue pathology. BMC Vet Res 2024; 20: 99.
24. Livak KJ, Schmittgen TD. Analysis of relative gene expression data using real-time quantitative PCR and the 2^−ΔΔCt method. Methods 2001; 25: 402-408.
25. Mohammadnejad K, Eslami M, Shahsavari S, Shamsi A. The effect of β-cryptoxanthin on testicular ischemia-reperfusion injury in a rat model. Iran Vet Sci Assoc J 2025; 20: 110-115.
26. El-Saadony MT, El-Sabagh M, Shaban SM, Mahmoud AWM, Abdel-Latif HMR, Ahmed AI, *et al*. Garlic bioactive substances and their therapeutic potential in inflammation and oxidative stress models. Front Immunol 2024; 15: 1277074.
27. Ghali R, Limam I, Kassrani I, Araoud M, Nouiri E, Fennira FBA, *et al*. LC-MS profiling and antioxidant, antifungal, and anticancer potentials of Tunisian *Allium sativum* L. extracts. PLoS

One 2025; 20: e0325227.
28. Soleimanzadeh A, Mohammadnejad L, Ahmadi A. Ameliorative effect of *Allium sativum* extract on busulfan-induced oxidative stress in mice sperm. Vet Res Forum 2018; 9: 265-2271.
29. Abouhamzeh B, Zare Z, Mohammadi M, Moosazadeh M, Nourian A. Bisphenol-S ınfluence on oxidative stress and endocrine biomarkers of reproductive system: A systematic review and meta-analysis. Int J Prev Med 2023; 14: 37.
30. Oberhaus SM. TUNEL and immunofluorescence double-labeling assay for apoptotic cells with specific antigen(s). Methods Mol Biol 2003; 218: 85-96.
31. Ulusoy Tangul S, Onat T, Aydoğan Kırmızı D, Doğanyiğit Z, Kaymak E, Oflamaz A, *et al*. Effect of bromelain on ischemia-reperfusion injury in the torsion model created in polycystic and normal ovarian tissues. Front Pharmacol 2025; 16: 1451592.
32. Soleimanzadeh A, Karvani N, Davoodi F, *et al*. Efficacy of silver-doped carbon dots in chemical castration: A rat model study. Sci Rep 2024; 14: 24132.
33. Logoyda LS, Abdel-Megied AM, Kondratova YM, Korobko DS, Abdel-Mageed WM. LC-MS/MS method development and validation for the determination of nifedipine in human plasma. Biointerface Res Appl Chem 2020; 10: 4971-4978.
34. Kalyoncu Ş, Yılmaz B, Demır M, Tuncer M, Bozdağ Z, İnce O, *et al*. Melatonin attenuates o onin attenuates ovarian ischemia r arian ischemia reperfusion injur fusion injury in rats by decreasing o easing oxidativ xidative stress index and per ess index and peroxynitrite. Turk J Med Sci 2020; 50: 1513-1522.
35. Zeynali E, Soleimanzadeh A, Azizi, S. Synergistic protection of alpha-glucosyl hesperidin and procyanidin against testicular ischemia-reperfusion injury. J Food Biochem 2025; 1: 1-18.
36. Zolfaghari S, Soleimanzadeh A, Baqerkhani M. The synergistic activity of fisetin on quercetin improves testicular recover in ischemia-reperfusion injury in rats. Sci Rep 2025; 15: 12053.
37. Behnejad G, Mohammadi T, Soleimanzadeh A. Allicin and hesperidin protect sperm production from environmental toxins in mice. Sci Rep 2025; 15: 14224.
38. Zhang M, Wu Y, Luo H. Ischemia–reperfusion injury: Molecular mechanisms and therapeutic interventions. Signal Transduct Targeted Ther 2024; 9: 12.
39. Öztürk AB, Kaya B, Yıldız S, Eren H. Investigation of the effects of silymarin on ovarian ischemia/reperfusion via Nrf2/HO-1/NQO1, Ki-67, and Wnt signaling pathways. J Biochem Mol Toxicol 2025; 39: e70138.
40. Qi D, Wang L, Zhou Y, Liu Y. Dimethyl fumarate protects against hepatic ischemia–reperfusion injury by alleviating ferroptosis via the NRF2/SLC7A11/HO-1 axis. Oxid Med Cell Longev 2023; 22: 818-828.
41.Kula H, Karadeniz M, Şimşek E. Effects of Allium cepa on ovarian torsion–detorsion injury in a rat model. Iran J Basic Med Sci 2023; 26: 577–584.